



Synthesis of polyacrylonitrile-co-sodium methallyl sulfonate copolymer (AN69) and polyacrylic acid (PAA) membranes for the removal of methylene blue from water

Chamekh M'Bareck¹ · Ely Cheikh S'Id^{1,2} · Abdelmoula Kheribech² · Abdelaziz Elouahli² · Zineb Hatim²

Received: 20 August 2019 / Revised: 31 October 2019 / Accepted: 14 November 2019 /

Published online: 22 November 2019

© Springer-Verlag GmbH Germany, part of Springer Nature 2019

Abstract

The scope of this work is focused on the removal of methylene blue (MB) from aqueous solution by adsorption (batch method) on polyacrylonitrile-co-sodium methallyl sulfonate copolymer (AN69) and polyacrylic acid (PAA) synthetic membranes which were prepared specifically for this purpose. Investigations have covered membrane properties and the determination of adsorption parameters. The immobilization of PAA chains into AN69 matrix was revealed by FTIR analysis, whereas the presence of small superficial microcavities was demonstrated by AFM scanning. Otherwise, the increase in PAA fraction (0 to 10%), in membrane composition, induces an increase in swelling ratio (12–22%) and ionic exchange capacity (0.8–1.2 meq/g). Moreover, the equilibrium adsorption capacity improves with the increase in alkalinity of initial adsorbate solution (pH=2–11) and with the concentration ($C=20\text{--}80\text{ mg/L}$). The results of kinetic adsorption show that the mechanism of adsorption is perfectly fitted by pseudo-second order ($R^2=0.999$) and the isotherm adsorption follows the Freundlich isotherm ($R^2=0.98$). From the different applied adsorption models, it was found that the maximum Langmuir adsorption capacity Q_m was 116 mg/g and the Freundlich index of adsorption n was 2.2.

Keywords Membrane · AN69 · PAA · Adsorption · Water treatment · Methylene blue

✉ Chamekh M'Bareck
chamec10@yahoo.com

¹ Research Unit: Polymères, Procédés Et Milieux Aquatiques (2PMA), BP. 5026, FST, University of Nouakchott, Nouakchott, Mauritania

² Laboratory of Water and Environment (Team: Biomaterials and Electrochemistry), FS, Chouaib Doukkali University, El Jadida, Morocco

Introduction

With the progress of industrialization and the demographic rapid increase, many countries are exposed to serious drinking water problems [1]. This precious source is rarely available and exposed to various contaminants even after its treatment. Toxic components not only affect the quality of supplied water but also the equilibrium of aquatic system and all environment compartments [2–5].

For many decades, adsorption processes were successfully used to resolve the deterioration of water quality which is caused by the presence of various contaminants such as dyes, phenols, pesticides, pharmaceutical drugs, and inorganic compounds [6]. Methylene blue (MB) is a toxic compound with low molecular weight [7–10]. Often, it is used as a model to test materials' efficiency in the removal of organic toxic compounds. In these recent years, different materials were tested to remove MB from aqueous solution. Abdelrahman et al. [11] used amorphous metallic products composed of sodium, silicon, iron, nickel, chromium, or zinc to remove MB from aqueous solution. These products lead to adsorption capacity ranging between 36.51 and 53.79 mg/g. Makhado et al. [12] revealed that the modification of the surface of Xanthan gum-cl-polyacrylic acid hydrogel permits a very high adsorption capacity of MB which was 521 mg/g. Yang et al. [13] tested the adsorption ability of synthesized κ -carrageenan/grapheme oxide gel by measuring the removal of MB from aqueous solution. The obtained results show high adsorption capacity, 658 mg/g, and excellent regeneration ability. Otherwise, He et al. [14] have prepared microscale biochar particles/polysulfone mixed matrix hollow fiber membranes which exhibited a high removal efficiency of methylene blue from water under wide pH range from 4 to 10. Others materials as tea waste were also proposed to remove MB from water [15]. Table 1 lists the maximum adsorption capacity for some products used recently in BM removal.

Here, novel AN69/PAA membranes were prepared for the removal of MB dye from aqueous solution. AN69 is an interesting anionic polymer with many engineering applications [16, 17]. It is a semicrystalline copolymer which contains strong negative sulfonate groups. It was successively used to synthesize hemodialysis membranes in spite of blood coagulation which is due to the adsorption of proteins onto membrane surface [18]. The incorporation of hydrophilic polymer was useful to prevent the coagulation process and to protect membrane surface against cell

Table 1 Comparison of adsorption capacity values for different adsorbents

Adsorbent	Adsorption capacity (mg/g)	References
Amorphous metallic products	36.51–53.79	[11]
Xanthan gum-cl-polyacrylic acid hydrogel	521	[12]
κ -carrageenan/grapheme oxide gel	658	[13]
Biochar particles/polysulfone	544	[14]
Tea waste	85	[15]
AN69/PAA	116	This work

adsorption [19, 20]. Therefore, the interest of AN69/PAA membranes, obtained by the incorporation of PAA in AN69 matrix, is not only limited to water treatment as presented here, but it can extend to other areas such as medical and health applications [21].

The determination of membrane properties has covered the measurement of swelling ratio (S_p), ionic exchange capacity (C_{exch}), topographic features (AFM), and functional groups identification (FTIR). These properties contribute in the understanding of membrane efficiency in adsorption process. The study of adsorption of MB dye has covering the effect of pH and initial concentration of adsorbate solution, the effect of membrane composition, and the analysis of results by the most known isotherm and adsorption kinetic models.

Materials and methods

Membrane synthesis

Polyacrylonitrile-*co*-sodium methallyl sulfonate copolymer (AN69) was supplied by Rhodia (France), whereas polyacrylic acid (PAA) and dimethyl formamide (DMF) were provided by Sigma-Aldrich (France). All polymers and chemical products were used as supplied, without any further purification. The molecular weight of PAA was 450,000 g/mol, and the molecular weight of methylene blue was 319.5, and its maximum absorption was at 650 nm.

AN69 was dissolved, 5 wt%, in dimethyl formamide (DMF) in a glass reactor equipped with a mechanical stirrer and thermostated at 90 °C for more than 3 h. Afterward, polyacrylic acid (PAA) was added to the AN69 in known proportions and stirred for 3 h to form the casting dopes. The dope was cast on a glass plate with a laboratory-made Gardner knife. The cast liquid film was dried in an oven at 60 °C for 1 h and finally immersed in a coagulation bath containing a sufficient volume of MilliQ water at 27 °C. The membranes were thoroughly washed with water and stored until their use.

FTIR spectrum recording

Before its mounting on the attenuated total reflection device for FTIR measurements, the films were dried in a vacuum oven at 70 °C for 12 h. The FTIR spectrometer was a Nicolet AVATAR 360 FTIR equipped with a Ge ATR crystal. The spectra were recorded at an incident beam angle of 45°. For each sample, the infrared spectrum is the result of 64 scans with a resolution of 4 cm⁻¹.

Atomic force microscopy

AFM imaging in the contact mode was done with a “Nanoscope II” from Digital Instruments™ (Santa Barbara, USA) using a 140-μm scanner. The cantilevers used were characterized by a spring constant of 0.06 N/m. A standard pyramidal

tip in silicon nitride was used. The measurements were carried out in air and at a constant force in the 10^{-9} to 10^{-8} N range.

Swelling ratio

The swelling ratio is usually determined to get an idea on the extension of membrane structure. It is related to the difference between the weights of membrane structure in swollen and dried state. The swelling ratio is calculated by the following formula:

$$Sr = \frac{W_s - W_d}{W_s}$$

where W_s is the weight of the swollen membrane and W_d the weight of the dried membrane.

Ionic exchange capacity

The ionic exchange process might be defined as a reversible exchange of ions between membrane and its liquid environment. This exchange takes place without substantial modification of membrane structure.

The ionic exchange capacity was determined after alternative sample conditionings in 0.1 M NaOH and 0.1 M HCl for an immersion time of at least 4 h. In H^+ form, the sample was equilibrated in water for at least 12 h to remove the free hydrogen ions and afterward immersed in NaCl 0.1 M for 4 h. The released H^+ ions in the NaCl medium were titrated by NaOH 0.01 M [22].

Adsorption of methylene blue

Batch adsorption of MB on AN69/PAA (95/05) was carried out in Erlenmeyer flasks with 25 mL of dye solution at room temperature (27 °C). The Erlenmeyer flasks containing membrane samples were agitated at constant speed 100 T/min for a known time. The range concentration of dye was between 20 and 80 $mg L^{-1}$.

The dye absorption was measured at the wavelength corresponding to the maximum absorption, $\lambda_{max} = 650$ nm, using a 6705 UV/VIS spectrophotometer, model Jenway.

The amount of dye adsorbed onto membrane Q_e (mg/g) was calculated as follows:

$$Q_e = (C_0 - C_e) V/m$$

where Q_e is the adsorbent amount of dye (mg/g) and C_0 ($mg L^{-1}$) and C_e ($mg L^{-1}$) are the initial and equilibrium concentrations of dye, respectively. m (g) is the mass of membrane sample. V (L) is the volume of the liquid phase.

Results and discussion

The phase inversion method is commonly used to prepare membranes. It is simple, and it permits the control of membrane performance [23, 24]. Here, AN69 and PAA polymers were mixed in known proportions to get ionic exchange membranes with excellent mechanical structure. AN69/PAA membranes show better mechanical properties when they are evaporated in an oven at constant temperature. In free air, the evaporation of membranes leads to brittle structures. Fourier transform infrared (FTIR), atomic force microscopy (AFM), swelling ratio (Sr), and ionic exchange capacity (IEC) were used to collect the main information which affects the adsorption efficiency.

Fourier transform infrared results

FTIR is a powerful technique which provides serious information about material composition. It is frequently used to discover the structural change associated with polymers mixing. Figure 1 shows the FTIR spectra of pure AN69 (0% PAA), AN69/PAA 95/05 (5% PAA), and AN69/PAA 91/09 (PAA 9%) blends in the interval 800–4000 cm^{-1} . The comparison of third spectrum shows the appearance of new peaks at 1706 cm^{-1} which was assigned to carbonyl groups (C=O stretching). The appearance of this peak, in which intensity increases with the increase in PAA, proves the incorporation of PAA chains into AN69 matrix which is also confirmed by the significant increase in the intensity of hydroxyl groups band (O–H stretching) observed at 3570 cm^{-1} .

Otherwise, the shift of sulfonate groups' peak from 1162 cm^{-1} in pure AN69 to 1178 cm^{-1} in AN69/PAA 90/10 may be interpreted as the results of nonintermolecular interactions between functional groups embedded in the both polymers.

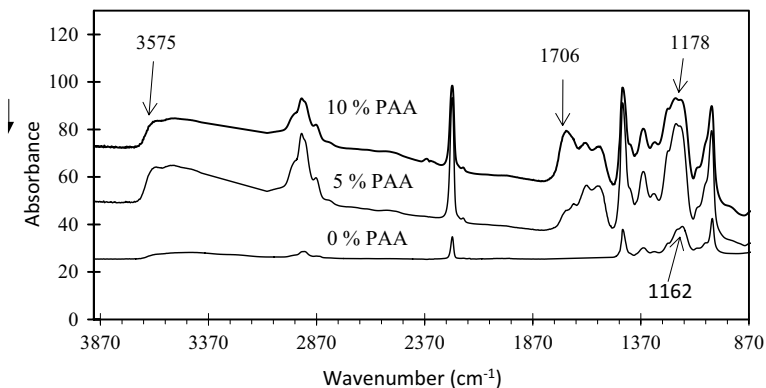


Fig. 1 FTIR spectrum of pure AN69 and AN69/PAA membranes

Atomic force microscopy results

The topographic images of AN69/PAA obtained by atomic force microscopy revealed the slight roughness of membranes' surface which increases with PAA percentage. The depth of the superficial microcavity might reach 250 nm as shown in topographic image of AN69/PAA 95/05 membrane, illustrated in Fig. 2. It might be noted that many researchers [10, 25] admitted that the adsorption of MB on materials depends largely on the chemistry of the adsorbent surface (ionic charges) than surface topographic. They consider the effect of materials' porous structure limited on this dye adsorption.

Swelling ratio and ionic exchange capacity

The results of swelling ratio show an increase in membrane swelling with the increase in PAA percentage. PAA is a hydrophilic polymer, so, its addition to AN69 improves the membrane swelling as shown in Table 3. Moreover, it appears that with the increase in PAA percent the ionic exchange capacity increases also.

It might be noted that the topographic images of AN69/PAA membranes obtained by AFM show an increase in the microcavities width with the increase in

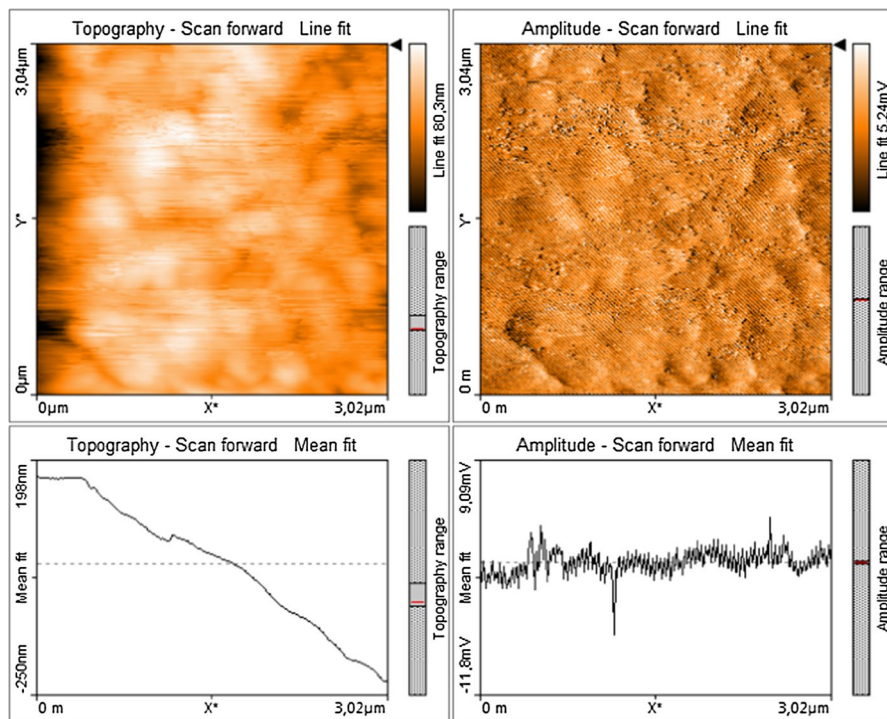


Fig. 2 AFM topographic images of AN69/PAA 95/05 membranes

PAA percentage. Otherwise, FTIR analysis proves the incorporation of PAA chains within AN69 matrix. Pure AN69 membrane shows the lowest swelling ratio and ionic exchange capacity. The little hydrophilicity of this polymer is due to sulfonate groups ($-\text{SO}_3^-\text{Na}^+$) dispersed along polymer chains. It enhanced significantly with the increase in PAA as this polymer added new hydrophilic groups (carboxylic groups).

Finally, it might be deduced that the results of FTIR analysis and AFM topographic images confirm the swelling ratios and ionic exchange capacity values. The incorporation of PAA polymer ($-\text{COOH}$) improves the amount of water contracted by membranes (S_r) and the ionic charges (IEC) which are mainly responsible for membrane hydrophilicity.

Adsorption of methylene blue

Effect of pH solution

The effect of pH on the adsorption of methylene blue on the AN69/PAA membrane was measured at different initial pH solutions as illustrated in Fig. 3. The adsorption percentage improves significantly with the increase in pH solution from lower values; afterward, the adsorption change is practically constant.

AN69/PAA membranes contain sulfonate groups ($-\text{SO}_3^-\text{Na}$) and carboxylic groups ($-\text{COOH}$) while MB contains positive charge. The increase in pH provokes an increase in carboxylic groups ionization mainly higher than $\text{pH}=5$. Thus, at lower pH, the adsorption of MB is mainly due to intermolecular interactions between sulfonate groups and MB positive charges, whereas, at higher pH, the improvement in intermolecular interactions is due to the implication of ionized carboxylic groups. Similar results were observed previously [12, 26–29]. Pavan et al. [26] found the same curve feature for the removal of MB from aqueous solution by adsorption using yellow passion fruit peel which contains superficial negative charges. Makhado et al. [12] proposed that the strong intermolecular interactions, observed at pH higher than 6, between hydrogel grafted with PAA and methylene

Fig. 3 Adsorption percent versus pH at $C=80$ mg/L, 150 rpm, and 298 °C

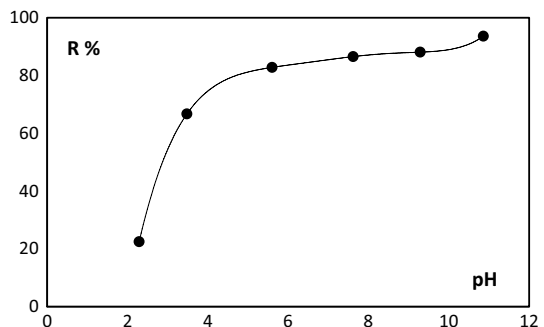


Fig. 4 Effect of the composition of AN69/PAA membrane on MB adsorption at pH = 10, $C = 80 \text{ mg/L}$, 150 rpm, 298 °C

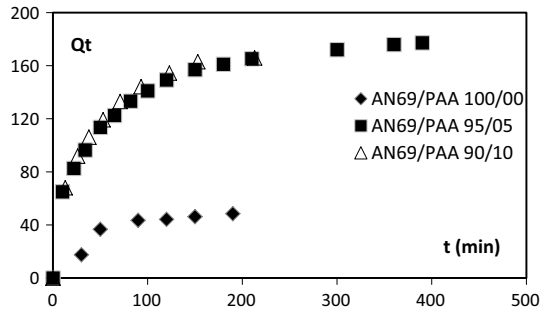
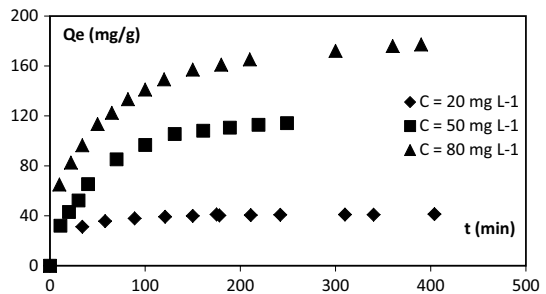


Fig. 5 Effect of initial concentration of MB solution on adsorption on AN69/PAA 95/05 membrane at pH = 10, 150 rpm, 298 °C



dye (MB) are due to the presence of negatively charged groups (COO^-) within hydrogel grafted and positives charges within MB.

Effect of membrane composition

Three membranes with different compositions 0, 5, and 10% of PAA were used to study the influence of polymer fraction on the adsorption of MB as shown in Fig. 4.

Curves of Fig. 4 show that the adsorption of MB increases significantly with the addition of PAA polymer. At pH = 10, all sulfonate and carboxylic groups are in ionized forms. Moreover, the addition of PAA to AN69 brings two advantages: the increase in ionic exchange capacity and the swelling ratio. These advantages contribute to the improvement in MB adsorption on AN69/PAA membrane. These results confirm that the incorporation of negative groups within membrane improves adsorption which is mainly due to establishment of ion–ion interactions between dye and AN69/PAA membrane [30]. This interpretation is in agreement with Peyratout et al. [31] results who assigned the adsorption of different cationic dyes on negative charged polyelectrolytes, in aqueous solution, to the establishment of electrostatic interactions between the positives charges of dye molecules and the negative sulfonate groups of polyelectrolyte.

Effect of initial concentration:

Three initial concentrations 20, 50, and 80 mg L⁻¹ of MB were used to follow the variation in adsorption in function of time as represented in Fig. 5.

At constant concentration, adsorption capacity increases sharply in the first minutes of contact and becomes practically steady afterward. In the first interval, interactions between dye molecules and membrane are strong due to the low saturation level of membrane sites. Then, the adsorption of dye molecules is rapid, whereas, in the second interval, where the adsorption seems to be steady, the decrease in intermolecular interactions between dye and membrane sites is due to the progressive saturation of these sites.

It appears clearly that with the increase in initial concentration, the adsorption capacity Q_t increases. This behavior might be explained as a result of the accumulation process of dye molecules surrounding membrane sites. It might be suggested that with the increase in dye molecules, in front of membrane sites, novel layers are formed. This analysis is based on the well-known process of layer-by-layer formation [31, 32].

Isotherm analysis

Langmuir, Freundlich, and Temkin models were used to collect more information about adsorption of MB dye onto AN69/PAA membrane surfaces [33, 34].

Langmuir’s model The Langmuir model is based on the following mathematical equation:

$$Q_e = Q_m K_L C_e / (1 + K_L C_e)$$

where Q_e is the amount of MB adsorbed per gram of the membrane at equilibrium (mg/g), C_e the equilibrium concentration of MB (mg/L), Q_m the maximum monolayer coverage capacity (mg/g), and K_L the Langmuir isotherm constant (L/mg).

The linearization of this equation leads to the following formula:

$$1/Q_e = 1/Q_m + 1/(K_L Q_m C_e)$$

Figure 6 presents the plot of $1/Q_e$ versus $1/C_e$ which leads to the determination of values of maximum monolayer coverage capacity (Q_m) and the Langmuir isotherm

Fig. 6 Plot of $(1/Q_e)$ versus $1/C_e$ for the adsorption of MB on AN69/PAA 95/05 membrane at pH= 10, C= 80 mg/L, 150 rpm, 298 °C

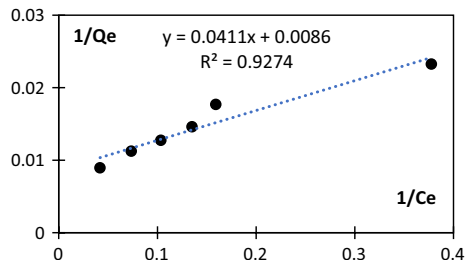
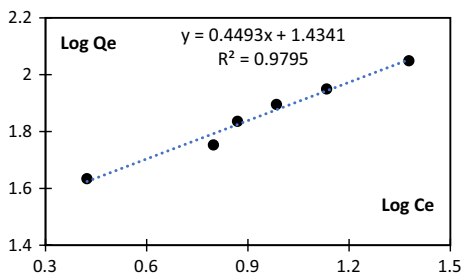


Fig. 7 Plot of $\text{Log } Q_e$ versus $\text{Log } C_e$ for the adsorption of MB on AN69/PAA 95/05 membrane at: pH=10, C=80 mg/L, 150 rpm, 298 °C



constant (K_L). This last parameter might be used to calculate the Langmuir separation factor (R_L) according to the following formula:

$$R_L = 1 / (1 + K_L C_0).$$

The adsorption is considered favorable when the value of R_L is between 0 and 1, linear if $R_L=0$, and unfavorable when the R_L values are greater than 1 [34].

The exploitation of this plot leads to $Q_m=116.27$ mg/g and $K_L=0.21$. The calculus of R_L leads to values ranging between 0.06 and 0.19 which are included between 0 and 1. Then, the adsorption of MB onto AN69/PAA membrane is favorable. But, it might be noted that the value of correlation coefficient is different from unit ($R^2=0.93$). Therefore, the Langmuir model does not fit this adsorption process perfectly.

Freundlich's model Freundlich has proposed an empirical model which follows the following equation:

$$Q_e = K_f C_e^{1/n}$$

where Q_e is the amount of dye adsorbed per gram of the membrane at equilibrium (mg/g) and C_e the equilibrium concentration of dye (mg/L).

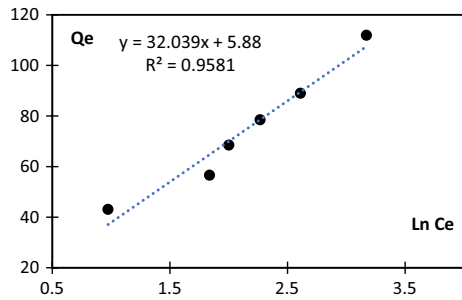
K_f is the adsorption capacity at unit concentration and $1/n$ is the adsorption intensity. Their values can be deduced from the linearization of the above equation:

$$\text{Log } Q_e = f (\text{log } C_e)$$

Adsorption is considered favorable when n value is higher than 1 and unfavorable if it is lesser than 1 [33, 34].

The calculation of n and K_f values, from the plot of the linearization of Freundlich's equation as shown in Fig. 7, leads to 2.22 and 4.19, respectively, while the correlation coefficient R^2 is equal to 0.98. From the value of correlation coefficient, it might be noted that Freundlich's model describes the adsorption of MB better than Langmuir's model does.

Fig. 8 Plot of Q_e versus $\ln C_e$ for the adsorption of MB on AN69/PAA 95/05 membrane at: pH= 10, C=80 mg/L, 150 rpm, 298 °C



Otherwise, the value of adsorption intensity, which is higher than 1, supports the establishment of intermolecular interactions between MB and AN69/PAA membrane as considered previously.

Temkin’s model The advantage of Temkin’s model is the prediction of adsorption heat (J/mol) and equilibrium bending constant (L/mg). This model is based on the following equation [33, 34]:

$$Q_e = (RT/b) \ln (K_t C_e)$$

where b is the adsorption heat (J/mol) and K_t is the equilibrium bending constant (L/mg).

The linearization of Temkin’s equation leads to the following formula:

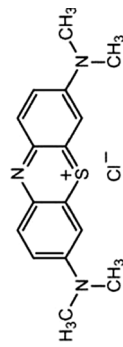
$$Q_e = (RT/b) \ln K_t + (RT/b) \ln C_e$$

From the plot of Q_e versus $\ln C_e$, we deduced the heat of adsorption ($b = 77.4$ kJ/mol) and the equilibrium bending constant ($K_t = 1.20$) as shown in Fig. 8.

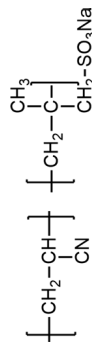
It might be deduced from different parameters, summarized in Table 2, that adsorption of MB on AN69/PAA is favorable. It seems to be in total conformity with Freundlich’s model which suggests the heterogeneity of membrane surface or/and the formation of different layers as proposed previously [32]. The microcavity structures shown by AFM technique confirm the heterogeneity of membrane’s surface predicted by Freundlich’s model. Ouradi et al. [23] assigned the retention of MB by the AN69 ionic polymer to electrostatic interactions between negative membrane charges (sulfonate groups) and positive dye molecules.

Kinetic analysis

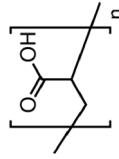
The mobility of adsorbate molecules from bulk solution toward adsorbent site is governed by the nature of interactions. To describe this mobility, three models are widely applied: (1) pseudo-first-order model proposed by Lagergren, pseudo-second-order model proposed by Mc Kay and Ho, and intraparticle diffusion model proposed by Weber and Morris [28, 35]. Here, adsorption of MB on AN69/PAA 95/05

Table 2 Chemical structures of MB, AN69, and PAA

Methylene blue structure (MB)



Polyacrylonitrile-co-sodium methallyl sulfonate copolymer structure (AN69)



Polyacrylic acid structure (PAA)

Fig. 9 Plot of $\ln (q_e - q_t)$ versus t for the adsorption of MB on AN69/PAA 95/05 membrane at: pH=10, $C=80$ mg/L, 150 rpm, 298 °C

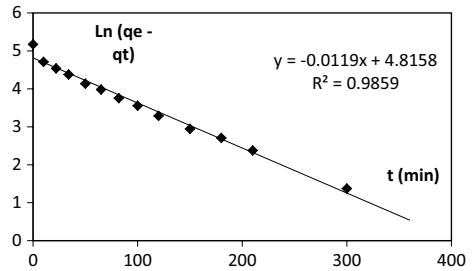
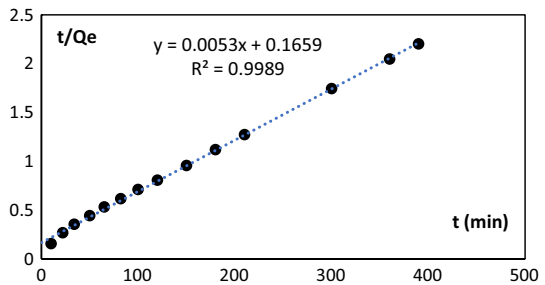


Fig. 10 Plot of t/Q_t versus t for the adsorption of MB on AN69/PAA 95/05 membrane at: pH=10, $C=80$ mg/L, 150 rpm, 298 °C



was studied under the following main conditions: initial concentration $C = 80$ mg/L, pH=10.

(a) Pseudo-first-order model: the linear form of pseudo-first order as proposed by Lagergren is given by the following equation:

$$\ln (q_e - q_t) = \ln q_e - K_1 t$$

where q_t and q_e are the capacities of adsorption at instant t and equilibrium time, respectively, and K_1 is the equilibrium rate constant (min^{-1}).

The exploration of kinetic results according to the pseudo-first-order model, as represented in Fig. 9, leads to a correlation coefficient $R^2 = 0.986$, adsorption rate constant of pseudo-first-order $K_1 = 0.0119 \text{ min}^{-1}$, and an equilibrium capacity equal to 123.4 mg/g. In spite of the correlation coefficient value, which is not so different from the unit, the value of theoretical equilibrium capacity is very different from the value of experimental one (177 mg/g).

(b) Pseudo-second-order model: the linear form of pseudo-second order as proposed by Mc Kay and Ho is given by the following equation:

$$t/q_t = 1/(K_2 q_e^2) + t/q_e$$

where q_t and q_e are the capacities of adsorption at instant t and equilibrium time, respectively, and K_2 is the equilibrium rate constant of the second-pseudo order (g min mg^{-1}).

The plot of t/q_e versus t , as shown in Fig. 10, leads to a value of correlation coefficient very close to unit $R^2 = 0.9989$. Moreover, the exploitation of plot data allows the determination of equilibrium capacity $q_e = 188$ mg/g and the

Fig. 11 Plot of Q_t versus $t^{1/2}$ for the adsorption of MB on AN69/PAA 95/05 membrane at: pH=10, $C=80$ mg/L, 150 rpm, 298 °C

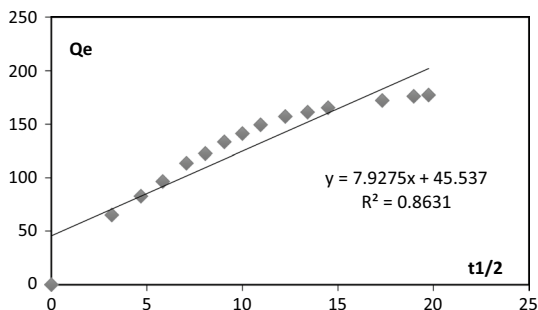


Table 3 Swelling ratio and ionic exchange capacity

Membrane	Composition	Swelling ratio (%)	Ion exchange capacity (meq/g)
AN69	100/00	11.00	0.84
AN69/PAA	95/05	14.00	1.14
AN69/PAA	90/10	22.00	1.26

Table 4 Factors of adsorption and correlation coefficients collected from Langmuir, Freundlich and Temkin models

Model	Langmuir	Freundlich	Temkin
Factor of adsorption evaluation	Separation factor $R_L=0.06$ and $0.19 < 1$	Adsorption intensity $n=2.2 > 1$	Heat of adsorption $b=77$ kJ/mol
Correlation coefficient	$R^2=0.93$	$R^2=0.98$	$R^2=0.96$

pseudo-second-order kinetic constant $K_2 = 1.7 \cdot 10^{-4}$. It might be noted that the theoretical equilibrium capacity is slightly higher than the experimental one (177 mg/g).

(c) Intraparticle model: the model proposed by Weber and Morris to describe the diffusion of adsorbate into adsorbent structure is given by the following equation:

$$q_t = K_i t^{1/2}$$

where q_t is the equilibrium adsorption at instant t and K_i is the equilibrium rate constant of intraparticle diffusion ($\text{mg/g min}^{1/2}$).

The plot of q_t versus $t^{1/2}$ as illustrated in Fig. 11 allows the determination of the values of correlation coefficient ($R^2=0.863$) and intraparticle diffusion constant ($K_i=0.1089$). It might be noted that the linear plot did not pass through the origin and the value of correlation coefficient is very different from 1. As a result, intraparticle diffusion model is not adequate to describe the kinetic of MB adsorption onto AN69/PAA 95/05 membranes.

Kinetic parameters, as summarized in Table 3, demonstrate that pseudo-second-order model leads to a value of correlation coefficient ($R^2=0.999$) very close to 1 and a theoretical equilibrium capacity ($Q_{e,\text{theo}} = 188$ mg/g), not so different from the

Table 5 Different values of kinetic parameters according to first pseudo-, second pseudo-orders and intraparticle models

Model	Pseudo-first order	Pseudo-second order	Intra-particle diffusion
K_i	0.01	$1.69 \cdot 10^{-4}$	0.11
Q_e (mg/g)	123.4	188	–
R^2	0.98	0.99	0.86

experimental one ($Q_{e.exp} = 177$ mg/g). Therefore, it can be considered as the most appropriate model to describe the mobility of MB molecules from solution bulk to AN69/PAA membranes' interface [29]. This kinetic order is due to the interactions between adsorbate molecules (positives charges) and adsorbent sites (negatives sites) (Tables 4, 5).

Conclusion

Novel synthetic membranes composed of polyacrylonitrile-*co*-sodium methallyl sulfonate copolymer (AN69) and polyacrylic acid (PAA) blends were prepared for the removal of methylene blue from aqueous solution. Fourier transform infrared technique was used to provide the immobilization of PAA polymer in the AN69 matrix, whereas the atomic force microscopy was employed to bring to fore the superficial membrane morphology: presence of microcavities. The tested AN69/PAA 95/05 membranes have ionic exchange capacities of 1.14 meq/g and swelling ratios of 14%. Based on the comparison of theoretical and experimental results and the value of correlation coefficient, the adsorption of MB follows perfectly Freundlich's model ($R^2 = 0.98$) and the kinetic of pseudo-second-order mechanism ($R^2 = 0.999$).

The intermolecular interactions between negative groups ($-\text{COO}^-$ and $-\text{SO}_3^-$), embedded into AN69 and PAA, and positive groups embedded into dye molecules are mainly responsible for the adsorption of MB onto AN69/PAA membranes. Moreover, this investigation leads to prove by AFM technique the heterogeneity of membrane surface predicted by Freundlich's model.

Acknowledgements Our thanks to Nouakchott El Assriya University in Mauritania and Chouaib Doukali University in Morocco. Hence, we would like to thank these universities for their support.

References

1. Levallois P (2006) Drinking water and public health: present and future challenges. *Rev Sci Eau* 19(2):127–135
2. Zani C, Feretti D, Buschini A, Poli P, Rossi C, Guzzela L, Caterino FD, Monarca S (2005) toxicity and genotoxicity of surface water before and after various potabilization steps. *Mut Res* 587:26–37
3. Watson SB, Lawrence J (2003) Drinking water quality and sustainability. *Water Qual Res J Can* 38:3–13

4. Antonio MT, Lopez N, Leret ML (2002) Pb and Cd poisoning during development alters cerebellar and striatal functions in rats. *Toxicology* 176:59–66
5. Varbanets MP, Zurbrugg C, Swarts C, Pronk W (2009) Decentralized systems for potable water and the potential of membrane technology. *Water Res* 43:245–265
6. E. Worch, *Adsorption Technology in Water Treatment* (2012) Walter de Gruyter GmbH & Co. KG, Berlin/Boston, Library of Congress (Germany)
7. Ait Ahsaine H, Zbair M, Anfar Z, Naciri Y, El haouti R, El Alem N, Ezahri M (2018) C ationic dyes adsorption onto high surface area almond shell activated carbon: Kinetics, equilibrium isotherms and surface statistical modeling. *Mat Tod Chem* 8:121–132.
8. Chen L, Ramadan A, Lü L, Shao W, Luo F, Chen J (2011) Biosorption of methylene blue from aqueous solution using *Lawn* grass modified with citric acid. *J Chem Eng Data* 56:3392–3399
9. Levin RL, Degrange MA, Bruno GF, Del Mazo CD, Taborda DJ, Griotti JJ (2004) Methylene blue reduces mortality and morbidity in vasoplegic patients after cardiac surgery. *Ann Thoracic Surg* 77:496–499
10. Deng H, Lu J, Li G, Zhang G, Wang X (2011) Adsorption Methylene Blue produced from cotton stalk on adsorbent materials. *Chem Eng J* 172:326–334.
11. Abdelrahman EA, Hegazy RM, El-Azabawy RE (2019) Efficient removal of methylene blue dye from aqueous media using Fe/Si, Cr/Si, Ni/Si, and Zn/Si amorphous novel adsorbents. *J Mater Res Technol*, in press
12. Makhado E, Pandeya S, Nomngongo PhN, Ramontja J (2018) Preparation and characterization of xanthan gum-cl-poly(acrylic acid)/ o-MWCNTs hydrogel nanocomposite as highly effective reusable adsorbent for removal of methylene blue from aqueous solutions. *J Colloid Interface Sci* 513:700–714
13. Yang M, Liu X, Qi Y, Sun W, Men Y (2017) preparation of κ-carrageenan/grapheme oxide gel beads and their efficient adsorption for methylene blue. *J Colloid Interface Sci* 506:669–677
14. He J, Cui A, Deng S, Chen JP (2018) Treatment of methylene blue containing wastewater by a cost-effective micro-scale biochar / polysulfone mixed matrix hollow fiber membrane: performance and mechanism studies. *J Colloid Interface Sci* 512:190–197
15. Uddin MdT, Islam MdA, Mahmud S, Rukanuzzaman Md (2009) Adsorptive removal of methylene blue by tea waste. *J Hazard Mater* 64:53–60
16. Tielemans C, Madhoun P, Lenaers M, Shandene L, Goldman M, Vanherweghem JL (1990) Anaphylactoid reactions during hemodialysis on AN69 membranes in patients receiving ACE inhibitors. *Kidney Int* 38:982–984
17. Peng FM (1985) Acrylonitrile polymers. In: Mark HF, Bikales NM, Overberger CG, Menges G (eds) *Encyclopedia of polymer science and engineering*, 2nd edition. Wiley, New York, p 1/426
18. Schetz M, Cromphaut SV, Dubois J, den Berghe GV (2012) Does the surface-treated AN69 membrane prolong filter survival in CRRT without anticoagulation? *Intensive Care Med* 38:1818–1825
19. Wang ZG, Wan LS, Xu ZK (2007) Surface engineering of polyacrylonitrile - based asymmetric membranes towards biomedical applications: an overview. *J Memb Sci* 304:8–23
20. Lin SC (1998) Protein's natural conformation and biomaterials' biocompatibility. *Chin Polym Bull* 1:1–10
21. Poitier J (2010) Feasibility between AN69 and Hemodiafiltration Online. *Néphrologie and Therapeutique* 6:21–27
22. Mbareck CO, Nguyen QT, Alaoui OT, Barillier D (2009) Elaboration characterization and application of polysulfone and polyacrylic acid blends as ultrafiltration membranes for removal of some heavy metals from water. *J Hazard Mater* 171:93–101
23. Ouradia A, Nguyen QT, Benaboura A (2014) Polysulfone–AN69 blend membranes and its surface modification by polyelectrolyte-layer deposit—Preparation and characterization. *J Memb Sci* 454:20–35
24. Lau WWY, Guiver MD, Matsuura T (1991) Phase separation in polysulfone/solvent/ water and polyethersulfone/solvent/water systems. *J Membr Sci* 59:219–227
25. Yenisoay-Karakas S, Ayguun A, Guunes M, Tahtasakal E (2004) Physical and chemical characteristics of polymer based spherical activated carbon and its ability to adsorb organics. *carbon* 42:477–484.
26. Pavan FA, Mazzocato AC, Gushikem Y (2008) Removal of Methylene Blue dye from aqueous solutions by adsorption using yellow passion fruit peel as adsorbent. *Biores Technol* 99:3162–3165
27. Hameed BH (2009) Removal of cationic dyes from aqueous solution using jackfruit peel as non conventional low cost adsorbent. *J Hazard Mater* 162:344–350

28. Demirbas E, Kobya M, Sulak MT (2008) Adsorption Kinetics of basic dye from aqueous solution onto apricot stone active carbon. *Biores Technol* 99:5368–5373
29. Selvam PP, Preethi S, Basakaralingam P, Thinakaran N, Sivasamy A, Sivanesan S (2008) Removal of Rhodamine B from aqueous solution by adsorption onto sodium montmorillonite. *J Hazard Mater* 155:39–44
30. Sanchez-Polo M, Rivera-Utrilla J (2002) Adsorbent-Adsorbate interactions in the adsorption of Cd(II) and Hg(II) on ozonized activated carbons. *Environ Sci Technol* 36:3850–3854
31. Peyratout C, Donath E, Daehne L (2001) Electrostatic interactions of cationic dyes with negatively charged polyelectrolytes in aqueous solution. *J Photochem Photobiol A Chem* 142:51–57
32. Shen JJ, Ren LL, Zhuang YY (2006) Interaction between anionic dyes and cationic flocculant P(AM-DMC) in synthetic solutions. *J Hazard Mater* 136(3):809–815
33. Yuh-Shan H (2003) Removal of copper ions from aqueous solution by tree fern. *Water Res* 37:2323–2330
34. Ferrandon O, Bouabane H, Mazet M (1995) Contribution à l'étude de la validité de différents modèles, utilisés lors de l'adsorption de solutés sur charbon actif. *Rev Sci Eau* 8:183–200
35. Renault F, Morin-Crini N, Gimbert F, Mari-Badot R, Crini G (2008) Cationized Starch Based Material as a new ion exchanger adsorbent for the removal of C: I acid blue 25 from aqueous solutions. *Biores Technol* 99:7573–7586

Publisher's Note Springer Nature remains neutral with regard to jurisdictional claims in published maps and institutional affiliations.